Guided Leak Detection in District Heating Networks from Aerial Thermal Imagery

Thomas Risch[1], Alexander Weidauer[2], Ahmad Hadavand[3*]

[1] Global Assistant & Logistic Group (GALG), CEO; on behalf of GeoFly GmbH, Business Development, Magdeburg, Germany - thomas.risch@galg-international.com
[2] Global Assistant & Logistic Group (GALG), Chief of Software Development and CTO, Germany - alex.weidauer@galg-international.com
[3] Persian Assistant & Logistic Group (PALG), CEO; Arak Science and Technology Park, Arak, Iran - hadavand@galg-persia.com

Keywords: Thermal Imagery, Aerial Imagery, District Heating, Leak Detection, Pipeline.

Abstract

Monitoring district heating networks, which distribute hot water or steam across urban areas, is a critical maintenance task. Aerial thermal infrared imagery offers an efficient tool for this purpose. Conventional detection of leakages in thermal raster data relies on data processing algorithms, but often suffers from false positives and missed detections. In this paper, we present a methodology for reliably detecting temperature anomalies—whether caused by actual leakages or by weak materials that may lead to future leakages—while minimizing false detections. Our approach generates auxiliary features to visually guide operators toward true detections. Specifically, we integrate thermal raster data with thermal isolines and statistical analyses that compare pipeline-axis temperatures to their surroundings. Cold pipeline segments are automatically omitted, while hot segments are highlighted according to their local temperature differences, thereby increasing the clarity and reliability of findings. To resolve ambiguities introduced by thermal hotspots near buildings or parking areas, we further incorporate Google Street View data for contextual verification. We evaluated the methodology on an airborne long-wavelength thermal dataset acquired over Nuremberg, Germany. Compared with conventional raster-based screening, our approach yielded a substantial improvement: the number of detected anomalies increased from 908 to 1,660, while the number of false positives was significantly reduced. An additional advantage of the proposed method is its ability to detect subtle temperature differences, enabling the identification of small but critical energy losses that might otherwise remain unnoticed.

1. Introduction

Satellite thermal remote sensing began in 1960 with the launch of TIROS-2, the first infrared radiometer (Harris, 2013). Interestingly, after five years, the first report on the observation of a thermal anomaly in a thermal image was published, in which an active lava flow field was detected. In thermal remote sensing, the emitted radiance from the surface of objects is measured and analyzed. This represents the fundamental difference between thermal and optical remote sensing, where the reflection of electromagnetic energy is measured and stored as data (Prakash, 2000).

The development of thermal sensors on various satellites continued across different countries and space organizations, resulting in sensors with improved quality and broader applications. Among the most notable and impactful missions are the NOAA AVHRR series, which began in 1978 with a ground sampling distance (GSD) of about 1 km, designed to monitor wildfires, as well as sea and land surface temperatures (Ehrlich et al., 1994). The Landsat series, starting from its fourth mission, included a thermal band with a GSD of around 100 m, aimed at supporting various environmental studies (Jimenez-Munoz et al., 2014).

Despite advances in satellite sensors in terms of temporal and spatial resolution, new applications could not overlook the advantages of aerial sensors. To the best of our knowledge, in parallel with the development of satellite thermal sensors, aerial alternatives attracted researchers for monitoring thermal anomalies on Earth and detecting fires (Hirsch, 1965). Thermal or infrared aerial imagery can be captured using sensors that include spectral bands in the thermal range of the electromagnetic spectrum or are specifically designed to capture energy in a single thermal band over a wider spectral range (Nguyen et al., 2021).

Thermal or infrared aerial images cover a wide range of applications from land and environment monitoring to hazard monitoring and security and surveillance (Sobrino et al., 2016). Thermal imagery is possible with both multi- and hyperspectral sensors which include bands in thermal wavelengths and single band thermal sensors. Depending on the nature of the project, the appropriate sensor should be selected. When the goal of the project is to detect different objects or study emissivity information, thermal bands with narrow bandwidth are more helpful, and sometimes these bands are used together with other spectral bands. However, for anomaly detection purposes, single-band thermal sensors provide more accurate details of the temperature of objects (Hook et al., 1992).

In this paper, we deal with leak detection in a district heating network, which is a kind of thermal anomaly detection. Single-band thermal sensors are helpful for handling this task. In the following, after a brief literature review, our sensor and dataset will be introduced. In the next section, the proposed algorithm

* Corresponding author

will be discussed. Then, the results will be presented, followed by the discussion and conclusions.

2. Literature Review

District heating networks distribute hot water from a central heating plant to end users, including residential buildings and industrial facilities. These networks consist of insulated underground pipes that extend throughout urban areas. Leakage is one of the major challenges, as it increases maintenance costs, leads to energy losses, and consequently reduces overall system efficiency. Technically, leakage detection methods can be classified into three categories (Zhou et al., 2018): physical model-based approaches, data-driven approaches, and unmanned airborne infrared thermography. Among these, airborne infrared thermography has demonstrated higher accuracy compared to the others, and as the technologies behind sensors and airborne platforms have matured, this method is receiving increasing attention in both research and practice.

Leakage along pipelines causes thermal anomalies that appear in aerial thermal images, and thresholding of recorded temperature values is a primary method for detecting potential leakage locations. Friman et al., (2013) introduced a method based on grouping pixels into small regions after thresholding thermal drone imagery acquired in the mid-wave infrared range. To address ambiguities caused by heat anomalies from buildings, they incorporated an edge-detection–based building detection algorithm to support the screening task and improve accuracy. Similarly, Berg & Ahlberg, (2014) applied a comparable method to aerial mid-wave infrared data, utilizing OpenStreetMap building footprints in their processing. In addition, they employed machine learning algorithms to reduce false detections and enhance the reliability of their results.

While machine learning and convolutional neural networks have gained popularity in recent years, comparing different algorithms remains attractive for some researchers. Hossain et al., (2020), examined eight different machine learning algorithms to detect leakage from UAV thermal imagery. By comparing CNNs with AdaBoost, variations of SVM, random forest, and several others, they concluded that CNN consistently outperformed the other algorithms.

A modification of the algorithm introduced by Friman et al., (2013) was later used to develop an open-source software tool for leak detection by Vollmer et al., (2023). They maintained the main structure of the algorithm but introduced changes to improve performance. For example, they incorporated 3D building models in LOD1 format and applied triangle histogram thresholding to detect thermal anomalies.

Despite the improvements in AI-based algorithms, model-driven approaches can still perform well with less complexity and lower computational demand. For instance, Vollmer et al., (2024) applied several anomaly detection algorithms to identify thermal leakage in district heating networks. They tested three methods: triangle histogram thresholding, local thresholding, and saliency mapping. Their results showed that local thresholding and saliency mapping were effective in producing robust results and detecting anomalies when the temperature difference between the leakage area and its surroundings was small. However, after vignetting correction, triangle histogram thresholding outperformed the other two algorithms.

In addition to its application in monitoring district heating networks, researchers have demonstrated that aerial thermography is capable of detecting leaks in underground water pipeline systems and can be considered a non-invasive testing method (Voysey and Campbell, 2023). Since leakage increases soil moisture and alters the heat capacity of the surrounding area, some researchers have investigated the potential of combining thermal infrared bands with other spectral bands to compute new indices, such as a water index, in order to improve pipeline leakage detection (Krapez et al., 2022).

Mitigating the influence of external thermal effects remains a persistent challenge when working with thermal infrared data. Vegetation cover, trees, water bodies, and shadows cast by elevated objects are major sources of interference. (Call et al., 2025) proposed simulating the effects of elevation and shadow caused by elevated objects using photogrammetrically generated DTM to achieve more precise leakage detection results.

3. Dataset

The dataset used in our experiments includes thermal aerial data and shapefile of thermal district network axis. Aerial data has captured by InfraTec ImageIR 8800 sensor. This sensor captures data in long wave infrared part of spectrum to benefit from more sensitivity and lower noise. More detailed information of the sensor is available in Table 1.

Sensor	Technical Specifications	
InfraTec ImageIR® 8800 	Spectral range	Long Wave (7.7 … 10.2) µm
	Detector format	640 x 512
	Readout mode	ITR
	Detector cooling	Stirling cooler
	Temperature measuring range	0.8
	82	(-40 ... 1,700) °C, up to 3,000 °C
	Measurement accuracy	± 1 °C or ± 1 %

Table 1- Specification of thermal aerial sensor

The sensor mounted on multi-engine aircraft to fulfil accuracy demands due to stable flight and guarantee safety measures flying over residential area. Aircraft equipped with precise GNSS antenna to guide pilot to move along the planned flight lines. A professional setup according to latest standards used in photogrammetry projects including precise IMU and GSM4000 stabilizer are used to prevent negative effect of aircraft movement and vibration on data quality. In Figure 1 equipment and setup of sensor and its peripherals are displayed.

Figure 1 - Professional system setup and equipment used in aerial mission

Before flight mission, flight plan conducted based on project requirements with enough forward and side overlap. Images captured with GSD of 30 cm over Nuremburg city which is in Bavarian state in southern Germany. Aerial mission conducted during night in March 2025. Using ground measurements during flight time the data has calibrated and photogrammetrically processed. Orthophoto mosaic generated for thermal district heating network of Nuremburg together with pipeline map prepared by the customer are depicted in Figure 2.

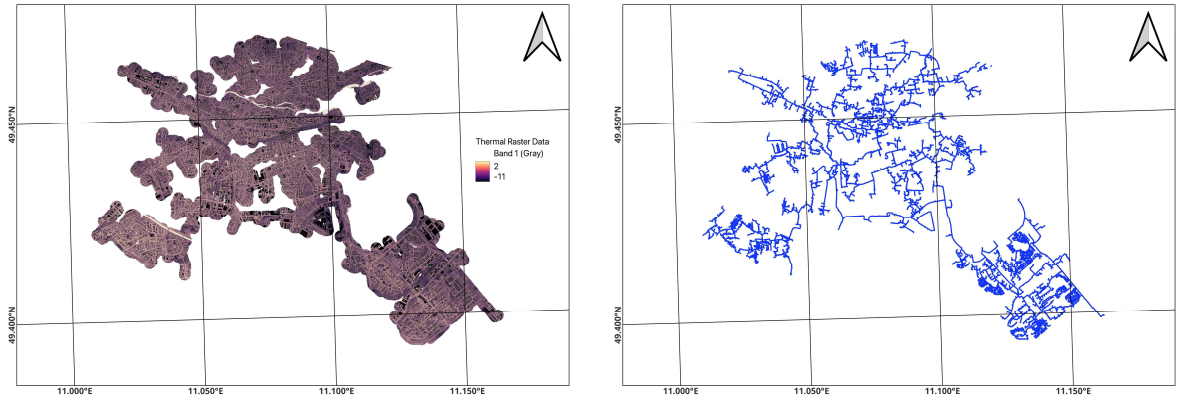

Figure 2 – Thermal orthomosaic (left) and district heating pipeline (right)

4. Methodology

The proposed method in this paper constitutes part of a larger project aimed at automating the procedure of pipeline leakage detection with the assistance of AI. At this stage, our objective is to empower screening operators to detect leakages with greater accuracy and to generate high-quality samples for training our dedicated AI model. To achieve this, we integrate thermal orthophotos with available vector layers and computed statistics and visualize them in a manner that guides screening operators toward actual leakage areas with a high level of confidence. The workflow of the proposed method is presented in Figure 3.

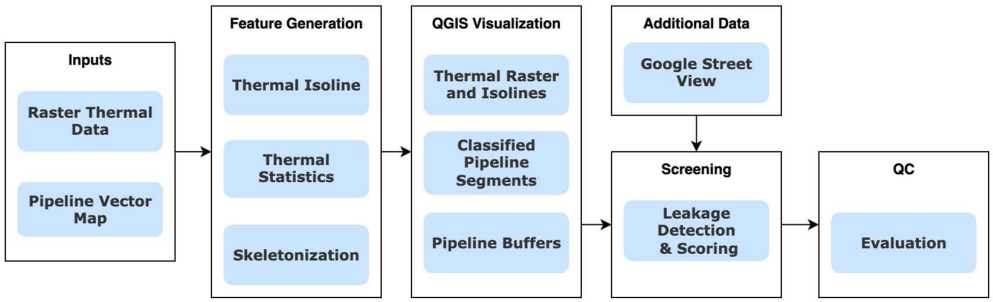

Figure 3 - Flowchart of proposed method

The inputs for our proposed method consist of a thermal raster image, which is geometrically processed into an orthomosaic of the study area, and a vector layer representing the pipeline. In the first step, we extract features from both input layers. From the vector layer, buffers are generated around the pipeline axis for different purposes, primarily to reduce computational costs: a 150-meter buffer is used to crop the orthomosaic, while 10-, 2-, and 0.3-meter buffers are employed for subsequent screening and to constrain the feature extraction process.

Next, thermal isolines are generated from the raster data. These contour lines, representing areas of equal temperature, are useful for detecting thermal anomalies and are produced within a 10-meter buffer around the pipeline axis.

Subsequently, to gain a better understanding and to provide a search and indexing space for the network structure, we devised an algorithm to convert the complex pipeline geometry provided by the customer into a generalized graph representing the network mid-axis. Given the complexity and large scale of the network, which extends across the entire city with numerous

hubs, junctions, and branches, the generalization of the pipeline into a mid-axis-based graph representation is not a straightforward task.

In a first pre-processing step, a unified buffer around the pipeline parts is generated to collect all technical structures within a certain radius (1 m) into a single corridor considered as a local region for investigating thermal signals. In the second step, the resulting corridor is reduced to the outer edges of the pipes to provide the geometry for mid-axis generation (skeletonization). Due to the large number of points and the complexity of the reduced corridor, a quad-tree-based vertex balancing is applied to make the calculation feasible in terms of runtime and memory consumption. In a post-processing step, partitioned results are merged into one mid-axis graph.

To support the user with classified hotspots along the pipeline, the mid-axis line was divided into segments of 0.5 m length. For each segment center point, thermal signature samples were drawn from the raster field within a 1 m radius, and local statistics (percentiles) were generated. To classify each sample, the median of the local statistic was compared against a global statistic derived from the local region above the pipeline.

To locate and delineate bounding boxes around each leakage along the pipeline, all relevant data were imported into QGIS. The thermal raster served as the background layer, while additional features—such as isolines and classified circles representing hotspots—were overlaid to facilitate the detection of actual leakages. Two additional map views were also set up in QGIS to display Google Earth satellite imagery and the OpenStreetMap layer available for the area, providing supplementary resources for better interpretation by the operator. In addition, when the pipeline passed near buildings, Google Street View data were used to verify whether a thermal anomaly was attributable to non-leakage sources such as garage doors, windows, or other structural elements.

The detected leakages are categorized into four classes according to our standard: Classes 1–3 correspond to true leakages of varying severity, whereas Class 4 represents anomalies outside the main network that cannot be ignored. Each finding is also scored based on visual and statistical assessment, with confidence levels designated as low, medium, or high. This confidence attribute supports optimal decision-making in network maintenance and provides valuable input for AI training. Although low-confidence findings may appear negligible, recording them remains crucial, as they can sometimes indicate early signs of future leakages that may escalate into high-confidence events.

Finally, the results are evaluated and compared with those obtained from operator-based screening methods that rely solely on the thermal raster.

5. Results

In this section, we will present the results obtained from each step of our flowchart in a visual form. This will demonstrate how our methodology can simplify leakage detection for operators. We will then provide quantitative results by comparing the findings of operators when relying only on the thermal raster and pipeline borders with their findings when assisted by our methodology.

In the following, we present an overview of a pipeline section with and without isolines and classified statistical overlays. After classifying the thermal statistics at nodes along the pipeline axis, only the five classes with the highest temperatures are displayed in the QGIS interface. This was done to highlight potential leakage areas for further review by operators. The shape and structure of the isolines provide an additional resource for determining whether a leakage has occurred. It is clear that experienced operators consider both thermal raster data and contextual information in their decision-making process. By comparing the left and right panels of Figure 4, it becomes evident that when operators rely solely on thermal raster data, the absence of texture in thermal imagery makes it difficult to confirm or reject anomalies. In contrast, the overlayed features we generated add valuable details and help visualize the thermal behaviour of different objects and temperature trends in the area. For example, the isolines in the figure highlight cars and manholes, while the classified thermal statistics (shown in yellow) indicate that the pipeline surroundings are warmer than their neighbourhood. In regions where no anomaly is present, no colour overlay is displayed.

This contribution has been peer-reviewed. The double-blind peer-review was conducted on the basis of the full paper.
https://doi.org/10.5194/isprs-annals-X-4-W8-2025-623-2026

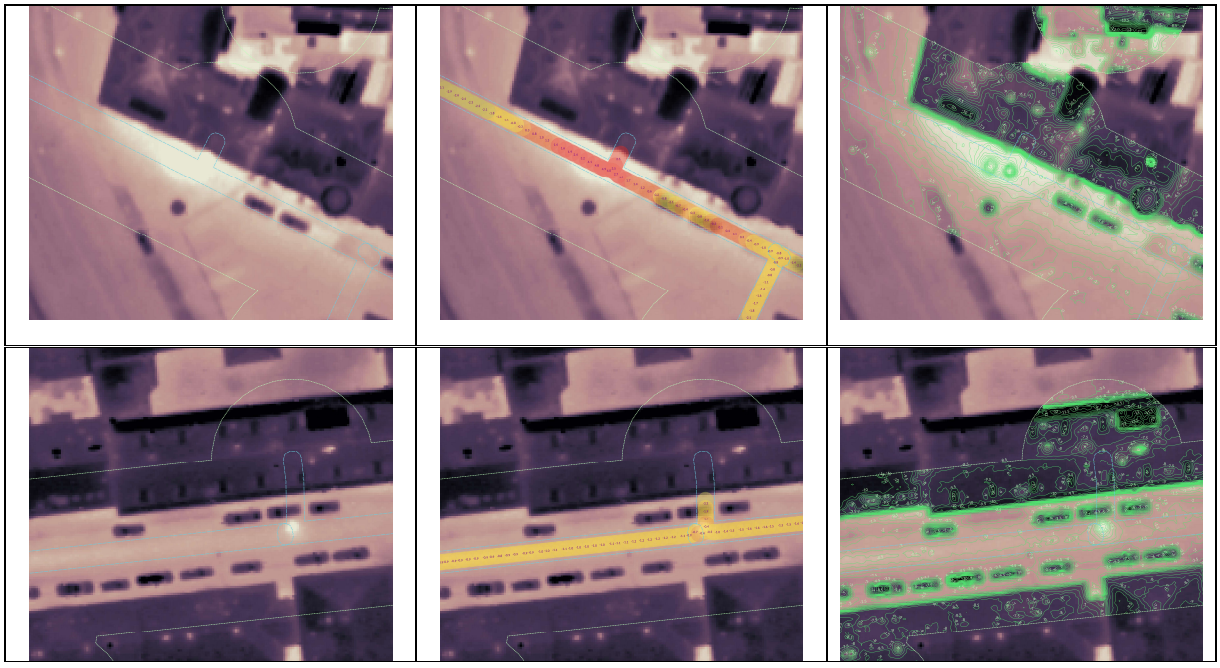

Figure 4 – thermal raster data and pipeline buffer (left), with thermal statistics (middle) and with isolines (right)

When considering potential leakages, isolines and thermal statistics often appear in distinctive patterns that guide us toward correct detections. As shown in Figure 5, leakages are typically surrounded by closed isoline forms, particularly in class 1 and class 2, where a significant amount of heat is being lost. For class 3, which is usually more difficult to detect, isolines also tend to form closed shapes, though they are less dense, or they may appear biased toward the pipeline axis.

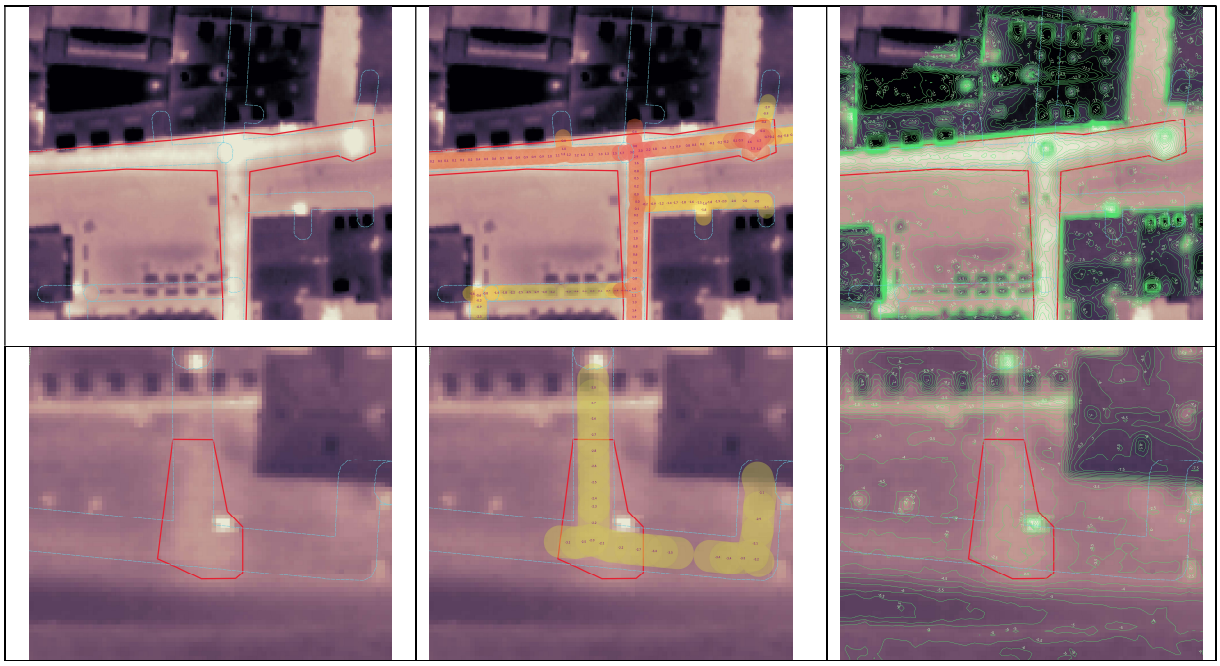

Figure 5 - Findings of class 2 (top) and class 3 (bottom) with and without isolines and thermal statistics

Despite the advantages of isolines and thermal statistics in detecting leakages, it is essential to consider contextual information to reduce the false positive rate. For this purpose, all signs should be carefully examined, and when needed, Google Street View data—readily accessible through Google Maps—can be used. As illustrated in Figure 6, sometimes closed-form isolines combined with thermal statistics indicate that an area is hotter than its surroundings. However, when contextual information is considered, it often reveals nearby buildings. Features such as garage doors, large windows, or glass facades typically cause thermal leakage from buildings, helping to avoid marking these false findings.

This contribution has been peer-reviewed. The double-blind peer-review was conducted on the basis of the full paper.
https://doi.org/10.5194/isprs-annals-X-4-W8-2025-623-2026 | © Author(s) 2026. CC BY 4.0 License.

Figure 6 - Hotspots visible in thermal raster and highlighted by isolines and thermal statistics (left), cross check of each area in Google Street View (right)

To validate the results, we compared the findings of two operators who independently performed screening using the proposed method. Their outputs were cross-checked by an expert in the field. We then compared these consolidated results with those obtained by another operator who conducted screening based solely on raster data and the 2D pipeline map. The evaluation was carried out on a 64-kilometre pipeline network.

The comparison between the two operators applying the proposed method showed an 80% agreement, indicating that both were able to successfully detect leakages. The results were then unified by the expert and compared against the operator who did not use our methodology.

The findings highlight a significant improvement: using our methodology, 1,660 potential leakage areas were identified, whereas only 908 areas were detected without it. Upon closer inspection, the expert determined that 384 of the 908 findings were false positives, meaning that without our methodology, 1,136 leakage sites went undetected. Most of these omissions corresponded to Class 3 leakages, which are difficult to detect but often evolve into more severe Class 2 or even Class 1 leakages over time.

6. Discussions and Conclusions

In this paper, we presented a methodology to assist operators in detecting and marking leakages in aerial thermal imagery. We used data over a large city, which is challenging to cover with drones. Leakage detection directly contributes to reducing energy waste and lowering maintenance costs of the network. In our proposed method, we employed isolines and thermal statistics to compare the temperature of the pipeline with its surrounding area and identify hot spots. The methodology was evaluated on a dataset of the district heating network in Nuremberg, Germany, and the results demonstrated the effectiveness of our approach compared to using only thermal raster data for screening.

Comparison of the findings from our proposed method with those from the conventional screening approach revealed numerous Class 3 leakages that were missed by operators who did not use our methodology. This represents a significant achievement, as Class 3 leakages correspond to pipeline locations with minor leaks and weak thermal signatures. The large number of detections in this category demonstrates that even small leaks can contribute substantially to the city's energy losses, and that identifying and repairing these defects can promote more sustainable energy management. Moreover, Class 3 findings are critical because they may develop into Class 2 or Class 1 leakages in the near future. Considering them not only enhances immediate detection but also supports predictive assessment of the pipeline network's future condition.

The level of automation in our methodology may appear low compared to machine learning–based algorithms. This was intentional, as we aimed to ensure reliability given the high maintenance costs associated with false positives, which would require excavation to repair pipelines. Another reason for maintaining a lower level of automation was to gather sufficient high-quality data to train our dedicated deep learning model for full automation in the next phase. To achieve this, it is necessary to integrate contextual information, such as the presence of buildings, gates, and vehicles, which can produce extra heat and potentially cause ambiguity in detecting true leakages.

As part of our future work, we are developing a deep learning model to enhance the level of automation. Since our current methodology already assigns a confidence level to each finding, the model will be designed to label detections along with their associated confidence levels. Another innovative direction we are pursuing is the modeling of external factors such as vegetation, trees, surface material, and pipeline material, in order to assign weights to the findings. This weighting function is expected to provide a more reliable interpretation of the network's condition and thereby support more effective long-term planning while reducing the number of false positive findings.

In addition, we plan to extend the use of thermal imagery to broader applications, including climate monitoring and the detection of leakages in gas and water pipeline networks. These networks, particularly in countries such as Iran, often suffer losses due to aging infrastructure, resulting in significant waste

of gas and water. Preventing these losses is therefore essential for the sustainable management of critical resources.

References

Berg, A., Ahlberg, J., 2014. Classifying district heating network leakages in aerial thermal imagery, in: Swedish Symposium on Image Analysis.

Call, L., Dasher, R., Xu, Y., Johnson, A.W., Dou, Z., Shafer, M., 2025. Elevation Models, Shadows, and Infrared: Integrating Datasets for Thermographic Leak Detection. Remote Sens (Basel) 17, 2399.

Ehrlich, D., Estes, J.E., Singh, A., 1994. Applications of NOAA-AVHRR 1 km data for environmental monitoring. Remote Sens (Basel) 15, 145–161.

Friman, O., Follo, P., Ahlberg, J., Sjökvist, S., 2013. Methods for large-scale monitoring of district heating systems using airborne thermography. IEEE Transactions on geoscience and remote sensing 52, 5175–5182.

Harris, A., 2013. Thermal remote sensing of active volcanoes: a user's manual. Cambridge university press.
Hirsch, S.N., 1965. Airborne infrared mapping of forest fires. Fire Technol 1, 288–294.

Hook, S.J., Gabell, A.R., Green, A.A., Kealy, P.S., 1992. A comparison of techniques for extracting emissivity information from thermal infrared data for geologic studies. Remote Sens Environ 42, 123–135.

Hossain, K., Villebro, F., Forchhammer, S., 2020. UAV image analysis for leakage detection in district heating systems using machine learning. Pattern Recognit Lett 140, 158–164.

Jimenez-Munoz, J.C., Sobrino, J.A., Skoković, D., Mattar, C., Cristobal, J., 2014. Land surface temperature retrieval methods from Landsat-8 thermal infrared sensor data. IEEE Geoscience and remote sensing letters 11, 1840–1843.

Krapez, J.-C., Sanchis Muñoz, J., Mazel, C., Chatelard, C., Déliot, P., Frédéric, Y.-M., Barillot, P., Hélias, F., Barba Polo, J., Olichon, V., 2022. Multispectral optical remote sensing for water-leak detection. Sensors 22, 1057.

Nguyen, T.X.B., Rosser, K., Chahl, J., 2021. A review of modern thermal imaging sensor technology and applications for autonomous aerial navigation. J Imaging 7, 217.

Prakash, A., 2000. Thermal remote sensing: concepts, issues and applications. International Archives of Photogrammetry and Remote Sensing 33, 239–243.

Sobrino, J.A., Del Frate, F., Drusch, M., Jiménez-Muñoz, J.C., Manunta, P., Regan, A., 2016. Review of thermal infrared applications and requirements for future high-resolution sensors. IEEE Transactions on Geoscience and Remote Sensing 54, 2963–2972.

Vollmer, E., Ruck, J., Volk, R., Schultmann, F., 2024. Detecting district heating leaks in thermal imagery: Comparison of anomaly detection methods. Autom Constr 168, 105709.

Vollmer, E., Volk, R., Schultmann, F., 2023. Automatic analysis of UAS-based thermal images to detect leakages in district heating systems. Int J Remote Sens 44, 7263–7293.

Voysey, D., Campbell, G., 2023. Assessing the detectability of underground water-pipe leaks with non-invasive technologies, in: Proc. Assoc. Public Auth. Surv. Conf. pp. 79–86.

Zhou, S., O'Neill, Z., O'Neill, C., 2018. A review of leakage detection methods for district heating networks. Appl Therm Eng 137, 567–574.